Influence of Sodium Carbonate Addition on Weight Loss of Bagasse Alkaline Black Liquor during Pyrolysis

Xusheng Li,[a,b,*] Jinlong Wang,[a,b] Derong Yan,[a,b] Yongjun Yin,[a,b] and Shuangfei Wang [a,b,*]

To understand the effects and the mechanism of sodium carbonate (Na_2CO_3) addition on the bagasse alkaline black liquor (BABL) pyrolysis, the reaction variables such as temperature, heating rate, and amount of Na_2CO_3 addition into BABL-solids were investigated under N_2 atmosphere from 50 °C to 1000 °C by thermogravimetic analysis (TGA). Scanning electron microscopy (SEM) and the Coats–Redfern method (CRM) were employed for surface microscopic morphology observations and kinetic analysis, respectively. The results showed that Na_2CO_3 plays an inhibiting and promoting role during devolatilization (200 °C to 650 °C) and the reduction stages (650 °C to 1000 °C), respectively. Adding Na_2CO_3 into BABL-solids tends to increase the thickness of the salt layer covering the BABL-solids surface, which increases the activation energy and reduces the weight loss ratio of BABL-solids pyrolysis within 200 °C to 650 °C. Adding Na_2CO_3 into the BABL-solids tends to increase the number of alkaline compounds or the active site of the reduction reaction, which reduces the activation energy and increases the weight loss ratio of BABL-solids pyrolysis within 650 °C to 1000 °C. The role of Na_2CO_3 as an additive could be well understood by studying the influence mechanism of Na_2CO_3 on BABL-solids pyrolysis.

Keywords: Bagasse; Alkaline black liquor; Pyrolysis; Kinetics; Sodium carbonate

*Contact information: a: Department of Light Industrial and Food Engineering, Guangxi University, Nanning, 530004, P.R. China; b: Guangxi Key Laboratory of Clean Pulp & Papermaking and Pollution Control, Nanning, 530004, P.R. China; *Corresponding author: lixusheng@gxu.edu.cn*

INTRODUCTION

In the pulp industry, more than 50 million tons of industrial lignin are present in black liquor each year (Lora 2008; Hubbe *et al.* 2019), and more than 95% of it is used as fuel for pulp mills to replenish energy and chemicals currently (Demuner *et al.* 2019). Thus, the recovery of additional energy and chemicals from black liquor is particularly important for pulp mills (Naqvi *et al.* 2010). Black liquor is treated *via* the Tomlinson recovery conventionally, which has been in existence for over 80 years. The traditional recovery process using the recovery boiler has proven to work well. However, the Tomlinson recovery boiler has several main disadvantages, including low electricity generation efficiency, emission of NO_x, SO_x, and particulate matter, as well as safety problems caused due to the salt melting during combustion (Gea *et al.* 2003; Naqvi *et al.* 2010). Therefore, new alternative methods are being intensively investigated to find more energy-saving, environmentally friendly, and user-friendly methods to control such processes (Li *et al.* 1991; Sricharoenchaikul *et al.* 2002). The gasification of black liquor has been widely investigated as alternatives to achieve electricity surplus based on satisfying the thermal and electrical needs of the pulp mills (Gea *et al.* 2005; Gustafsson and Richards 2009;

Huang and Ramaswamy 2011; Farzaneh *et al.* 2014). Black liquor gasification can be divided into three stages: drying, coking, and char gasification (Li *et al.* 1990). Essentially the drying of black liquor is a dewatering process; coking of black liquor can be considered as a devolatilization process; and char gasification is related to the catalysis of Na_2CO_3 (Gea *et al.* 2005). Although originally sodium is present as both organic and inorganic compounds in black liquor, it has been shown that all organic bound sodium is converted into Na_2CO_3 during pyrolysis before the temperature rises to 675 °C (Li *et al.* 1990).

The Na_2CO_3 is one of the important catalysts for biomass reactions (Nguyen *et al.* 2016; Yu *et al.* 2018), vegetable oil (Yigezu and Muthukumar 2014; Abdelfattah *et al.* 2018), and coal (Peng *et al.* 2017). There are very interesting results in the literature, which suggests that the addition of Na_2CO_3 to biomass pyrolysis has two opposite effects, namely promoting and inhibiting the pyrolysis process (Gea *et al.* 2002; Yu *et al.* 2018). The Na_2CO_3 promotes the gasification of hemicellulose significantly, however, inhibits the gasification of cellulose, lignin, straw, and pine (Yu *et al.* 2018). There is only limited available information to understand the mechanism of the two effects of Na_2CO_3.

Although several theories have been proposed to explain the role of Na_2CO_3 in the black liquor pyrolysis (Gea *et al.* 2005; Guo *et al.* 2012). Unfortunately, the effects of adding additional Na_2CO_3 on the pyrolysis of black liquor was not well investigated. It could be the presence of Na_2CO_3 in the alkaline black liquor itself. The influence of additional addition of Na_2CO_3 on the pyrolysis of black liquor has been neglected for a long time.

In this work, to reveal the influence mechanism of additional Na_2CO_3 on bagasse alkaline black liquor (BABL)-solids pyrolysis, the effects of the reaction variables (temperature, heating rate, and Na_2CO_3 amount into BABL-solids) on the weight loss rate and the weight loss ratio of BABL-solids pyrolysis were investigated by thermo-gravimetric analysis (TGA). Scanning electron microscopy (SEM) and Coats–Redfern method (CRM) were employed to observe the microscopic morphology and kinetics analysis, respectively. A better understanding to the role of Na_2CO_3 as an additive of BABL-solids pyrolysis could be achieved based on this study on the influence mechanism of Na_2CO_3 on BABL-solids pyrolysis.

EXPERIMENTAL

Materials and Methods

Materials

The BABL was obtained from the Guangxi Tianyang Nanhua Paper Industry Co. Ltd. (Baise, China). Various chemicals and reagents used in the experiment (including Na_2CO_3), were all analytically pure reagents purchased from Nanning Blue Sky Experimental Equipment Co. Ltd. (Nanning, China).

Experimental procedure

First, the original black-liquor was concentrated in a 2-L glass beaker by continuous stirring on a heating plate until its solid content reached over 60%. Secondly, the concentrated liquor was spread on a glass plate with a thickness of 1.0 mm to 3.0 mm and allowed dry in an oven at 105 °C for 48 h. The drying process needs to be gradual and

carefully controlled as possible to avoid the inhomogeneous distribution of inorganic compounds in the solid matrix. Any difference in the distribution would affect the final weight loss ratios and the weight loss rates, as shown in the following sections. After drying, the BABL-solids was ground and sieved through a 200-mesh sieve.

The ultimate and component analyses (wt.% of dry basis) were as follows: Na - 17.82%; K - 1.57%; C - 36.44%; H - 3.76%; N - 0.04%; S - 0.98%; Cl - 3.38%; Others were 36.0%. The organic and inorganic materials of BABL determined by the combustion method accounted for 69.04% and 30.96%, respectively. The elemental analysis was obtained in a CHNS Carlo Erba elemental analyzer (Model EA3000, EuroVector, Italy). The metal analysis was performed by atomic absorption after previous alkaline fusion (Model EasyLyte PLUS, Medica, Bedford, MA, USA). The chlorine analysis was obtained in Jana halogen analyzer (Model Multi X 2500, Jena, Germany).

The BABL-solids were pyrolyzed in a thermogravimetric analyzer (TGA, STA-449-F5, Netzsch, Bavaria, Germany). The sketch of TGA is shown in Fig. 1. Firstly, Na_2CO_3 (0%, 5%, 10%) is mixed with black liquor and subjected to the previous drying, grinding, and screening process. Then, 10 mg of BABL-solids powder were added to high-purity alumina (99.8%) flat pan; the gas flow of N_2 (99.99%) was adjusted to 60 cm^3 per min and held at 50 °C for 30 min before starting to warm up. Subsequently, the furnace temperature was increased from 50 °C to 200 °C, 400 °C, 600 °C, 700 °C, 800 °C, or 1000 °C at the selected heating rates of 10 °C, 20 °C, 30 °C, or 40 °C per min, respectively.

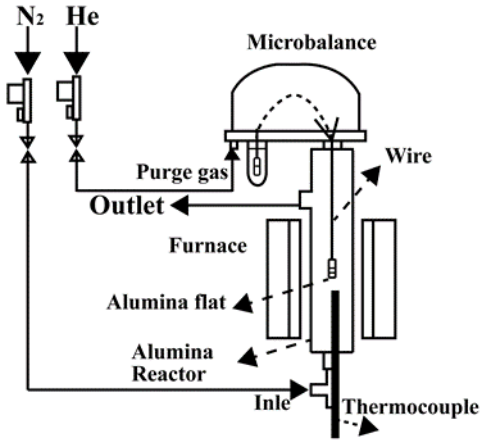

Fig. 1. Sketch of TGA

Surface Morphology observation

To further understand the influent mechanism of Na_2CO_3 on BABL-solids pyrolysis, SEM was adopted to investigate the surface morphology after the pyrolysis; 10% Na_2CO_3 was added into BABL and subjected to the previous drying, grinding, and screening process. Then, 10 mg of BABL-solids powder were added to the pan, and the gas flow of N_2 was adjusted to 60 cm^3 per min. It was held at 50 °C for 30 min before starting to warm up. The furnace temperature was increased from 50 °C to 200 °C, 400 °C, 600 °C, 700 °C, or 800 °C at the heating rates of 10 °C per min. The sample was kept at 200 °C, 400 °C, 600 °C, 700 °C, and 800 °C for 60 min and then cooled to room temperature. SEM was performed using SU8220 (Hitachi, Japan), and the sample was coated with gold spraying prior to the microscopic observation.

Calculation methods

In this work, the effects of important variables on BABL-solids pyrolysis, including the final pyrolysis temperature, heating rate, and Na_2CO_3 addition into the BABL-solids, were evaluated by analyzing the weight loss ratios and weight loss rates.

The weight loss ratio (r) is defined using Eq. 1 as follows,

$$r\ (\%) = \frac{m_0 - m_t}{m_0} \times 100 \quad (1)$$

where m_0 (mg) denotes the initial solid mass and m_t (mg) is the remaining solid mass at time t (min).

The weight loss rate (α) is defined as the variation of the weight loss ratio with time, according to Eq. (2),

$$\alpha = -\frac{\mathrm{d}r}{\mathrm{d}t} \quad (2)$$

Kinetic models

To understand the mechanism of the BABL-solids pyrolysis, CRM (Coats–Redfern method) was employed for kinetic analysis (Ebrahimi-Kahrizsangi and Abbasi 2008; Naqvi *et al.* 2015). The rate equation of BABL–solids pyrolysis can be expressed as follows,

$$\frac{\mathrm{d}\beta}{\mathrm{d}t} = \mathrm{K}(1-\beta) \quad (3)$$

where $\beta = \frac{m_0 - m_t}{m_0 - m_\infty}$ (%).

When combined with the Arrhenius equation (Jensen 1985; Song *et al.* 2015), Eq. 4 was obtained,

$$\frac{\mathrm{d}\beta}{\mathrm{d}t} = (1-\beta)A\exp\left(-\frac{E}{RT}\right) \quad (4)$$

where A represents the frequency factor (L/s), E represents the activation energy (kJ/ mol), and R is the ideal gas constant (R = 8.314 J/mol).

If the heating rate (γ) is constant, *i.e.*, $\gamma = \frac{\mathrm{d}T}{\mathrm{d}t}$, then

$$\frac{\mathrm{d}\beta}{\mathrm{d}T} = (1-\beta)\frac{A}{\gamma}\exp\left(-\frac{E}{RT}\right) \quad (5)$$

Integrating the equation by the Coats–Redfern method,

$$\ln\left[\frac{-\ln(1-\beta)}{T^2}\right] = \ln\left[\frac{AR}{\gamma E}\left(1-\frac{2RT}{E}\right)\right] - \frac{E}{RT} \quad (6)$$

If the value of E is very large in the general reaction area, the value of $\frac{2RT}{E}$ would be much smaller than 1. Therefore, $\ln\left[\frac{AR}{\gamma E}\left(1-\frac{2RT}{E}\right)\right]$ can be approximated to $\ln\left[\frac{AR}{\gamma E}\right]$. By plotting $\ln\left[\frac{-\ln(1-\beta)}{T^2}\right]$ against $\frac{1}{T}$, the slope, $-\frac{E}{R}$, and intercept, $\ln\left[\frac{AR}{\gamma E}\right]$, can be obtained and used to calculate the activation energy E and frequency factor A.

RESULTS AND DISCUSSION

TGA of BABL-Solids Pyrolysis

Effects of temperature on the weight loss of BABL-solids pyrolysis

The weight loss of black liquor pyrolysis can be divided into three stages: dewatering, devolatilization, and catalytic gasification. Figure 2 (A) and (B) displayed the relation of *α vs.* temperature and *α vs. r,* respectively. The associated data for the key nodes in two graphs were recorded in Table 1. The value of *α* is -0.15 %/min, -0.09 %/min, and -0.01 %/min at 166 °C, 543 °C, and 1000 °C, respectively (Table 1), which are nearly approaching zero. These temperatures are taken as nodes for the following analysis：

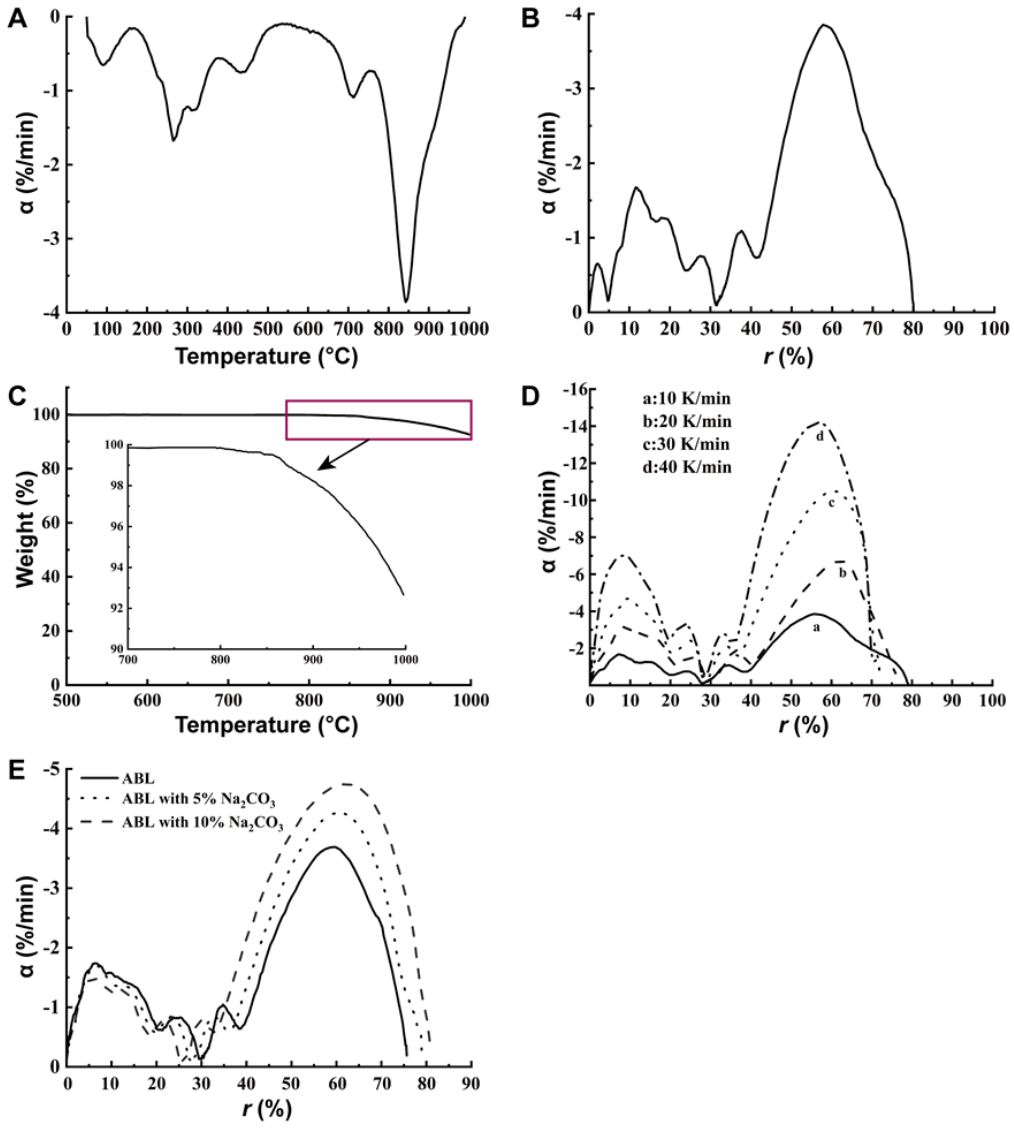

Fig. 2. TGA diagram of BABL-solids pyrolysis: (A) is *α vs.* temperature at 10 K/min; (B) is *α vs. r* at 10 K/min; (C) is TG of Na_2CO_3 at 10 K/min; (D) is *α vs. r* at 10, 20, 30, and 40 K/min; (E) is *α vs. r* with 0%, 5%, and 10% Na_2CO_3 addition into BABL-solids at 10 K/min

Table 1. Values of *α* and *r* of BABL-solids Pyrolysis from the Peaks and Valleys Observed in Fig. 2 (A) and (B)

α (%/min)	*r* (%)	Temperature (°C)	Remarks
-0.65	2.07	98	Valley
-0.15	4.68	166	Peak
-1.68	11.59	272	Valley
-1.21	16.55	307	Peak
-1.27	17.77	319	Valley
-0.56	23.85	383	Peak
-0.76	27.40	438	Valley
-0.09	31.40	543	Peak
-0.25	33.22	650	
-1.10	37.62	720	Valley
-0.73	42.28	770	Peak
-3.86	57.74	850	Valley
-0.01	80.07	1000	The end

(1) The *r*-value of BABL-solids is 4.68% within 50 °C to 166 °C. The weight loss can be attributed to dewatering from BABL-solids (Zhenqiu and Kefu 2000).

(2) The *r*-value of BABL-solids is 26.72% (increasing from 4.68% to 31.40%) from 166 °C to 540 °C. The weight loss can be explained by the devolatilization from the cracking of organic compounds (Beis *et al.* 2010). There are at least three valleys with *α*-value of -1.68 %/min, -1.27 %/min, and -0.76 %/min at 272 °C, 319 °C, and 438 °C respectively, as shown in Fig. 2 (A). Each valley implies an accelerated stage determined by the cracking of various organic compounds (Chu *et al.* 2017). These organic compounds present in BABL-solids, may include oligosaccharides (200 °C to 260 °C) (Evans and Milne 1988), cellulose (240 °C to 350 °C) (Bradbury *et al.* 1979), aliphatic carboxylic acids (200 °C to 300 °C) (Alén *et al.* 1995), and alkali lignin (400 °C to 550 °C) (Li and Wu. 2014), are fragmented into small molecules, which can be easily lost at the temperature range resulting in weightlessness at this stage.

(3) The *r*-value of BABL-solids is 48.67% (increasing from 31.40% to 80.07%) from 543 °C to 1000 °C, which includes a slow weight loss stage with *r*-value of BABL-solids of 1.72% from 543 °C to 650 °C. It can be explained by dehydrogenation with less weight loss (Gea *et al.* 2005). There is evidence in the literature that there is little cracking of organic compounds occurs over about 670 °C (Bradbury *et al.* 1979). Thus, the weight loss is attributed to release of CO from the reduction of some mixture of alkaline compounds with the carbon present in BABL-solids char within 650 °C to 1000 °C (Li and Van Heiningen 1990). These mixtures come mainly from the reduction of Na_2CO_3 with the carbon, but also, to some extent, from the pyrolysis of organic compounds present in BABL-solids such as carboxylates and phenolates of sodium (Guo *et al.* 2011). It has been shown that the weight of Na_2CO_3 decreased when the temperature was over 800 °C during pyrolysis (Whitty *et al.* 2008). Figure 2 (C) also showed this phenomenon. The weight of Na_2CO_3 was reduced by about 7.3% during the temperature range of 800 °C to 1000 °C, as shown in Fig. 2 (C). Thus, the weight loss can be explained by the removal of CO and Na_2CO_3 escaping during 650 °C to 1000 °C.

Therefore, it can be considered that the BABL-solids pyrolysis would be divided into

three stages according to the weight loss in the temperature ranges (50 °C to 166 °C, 166 °C to 650 °C, and 650 °C to 1000 °C).

Effects of heating rate on the weight loss of BABL-solids pyrolysis

When there is no change in the *r*-value, a decrease in the devolatilization and reduction stages were observed with the increase in heating rate as shown in Fig. 2 (D). It was attributed to the shortened residence time and the same final temperatures with the increasing of heating rate. The no change *r*-value can be explained by the minimum time, required to complete the maximum weight loss, less than the heating time, determined by these heating rates (10, 20, 30, and 40 K/min). This indicated that the devolatilization stage of BABL-solids pyrolysis is a fast weight loss process. Besides the decrease in *r*-value can be explained by the minimum time, required to complete the maximum weight loss, which is more than the heating time determined by these heating rates (10, 20, 30, and 40 K/min). This indicated that the reduction stage of BABL-solids pyrolysis as a slow weight loss process. It is clear that the decrease of the final *r*-value is due to the decrease of the reduction stage.

The α-value increased with the increasing heating rate as show in Fig. 2 (D). According to the definition of α, its value depends on *r* and the residence time in some stages. The α-value increase was attributed to no change in *r* and the shortened residence time with the increase of heating rate in the devolatilization stage of BABL-solids pyrolysis. The α-value increase with the increasing heating rate was attributed to the variation amplitude of *r* being smaller than the variation amplitude of residence time, as determined by heating rates in the reduction stage.

Effects of Na_2CO_3 addition on the weight loss of BABL-solids pyrolysis

Both α and *r* decreased with the increase in Na_2CO_3 ratio in the devolatilization stage, as shown in Fig. 2 (E). The percentage decrease of *r*-value were 29.98%, 27.67%, and 25.49% with 0%, 5%, and 10% Na_2CO_3 addition ratio, respectively from 200 °C to 543 °C. This indicated that the weight loss process in the devolatilization stage of BABL-solids pyrolysis could be inhibited by Na_2CO_3 addition. Both α and *r* increased with the increase of Na_2CO_3 addition ratio in the reduction stage: *r*-value were 45.64% (increasing from 29.98% to 75.62%), 51.13% (increasing from 27.67% to 79.00%), and 55.74% (increasing from 25.49% to 81.23%) from 543 °C to 1000 °C with 0%, 5%, and 10% Na_2CO_3 addition, respectively. This indicated that Na_2CO_3 addition could promote the weight loss of BABL-solids pyrolysis in the reduction stage.

Kinetics Analysis

The value for $\ln\left[\frac{-\ln(1-\beta)}{T^2}\right]$ and $\frac{1}{T}$ within 217 °C to 360 °C, 360 °C to 527 °C, 527 °C to 650 °C, 650 °C to 770 °C, and 770 °C to 900 °C displayed a good linear correlation from Fig. 3. The linear correlation coefficient (R^2) were greater than 0.99. According to Eq. 6, the values of $-\frac{E}{R}$ are the slope values of the fitting lines, then E-values of BABL-solids pyrolysis can be calculated, which were displayed in Table 2. The value of *E* of BABL-solids pyrolysis after adding 10% Na_2CO_3 into BABL-solids increased by 12.94%, 2.19%, and 28.27% within 217 °C to 360 °C, 360 °C to 527 °C, and 527 °C to 650 °C, respectively, as shown in Table 2. This result indicated that the weight loss of BABL-solids

pyrolysis is inhibited by Na_2CO_3 addition within these temperature ranges.

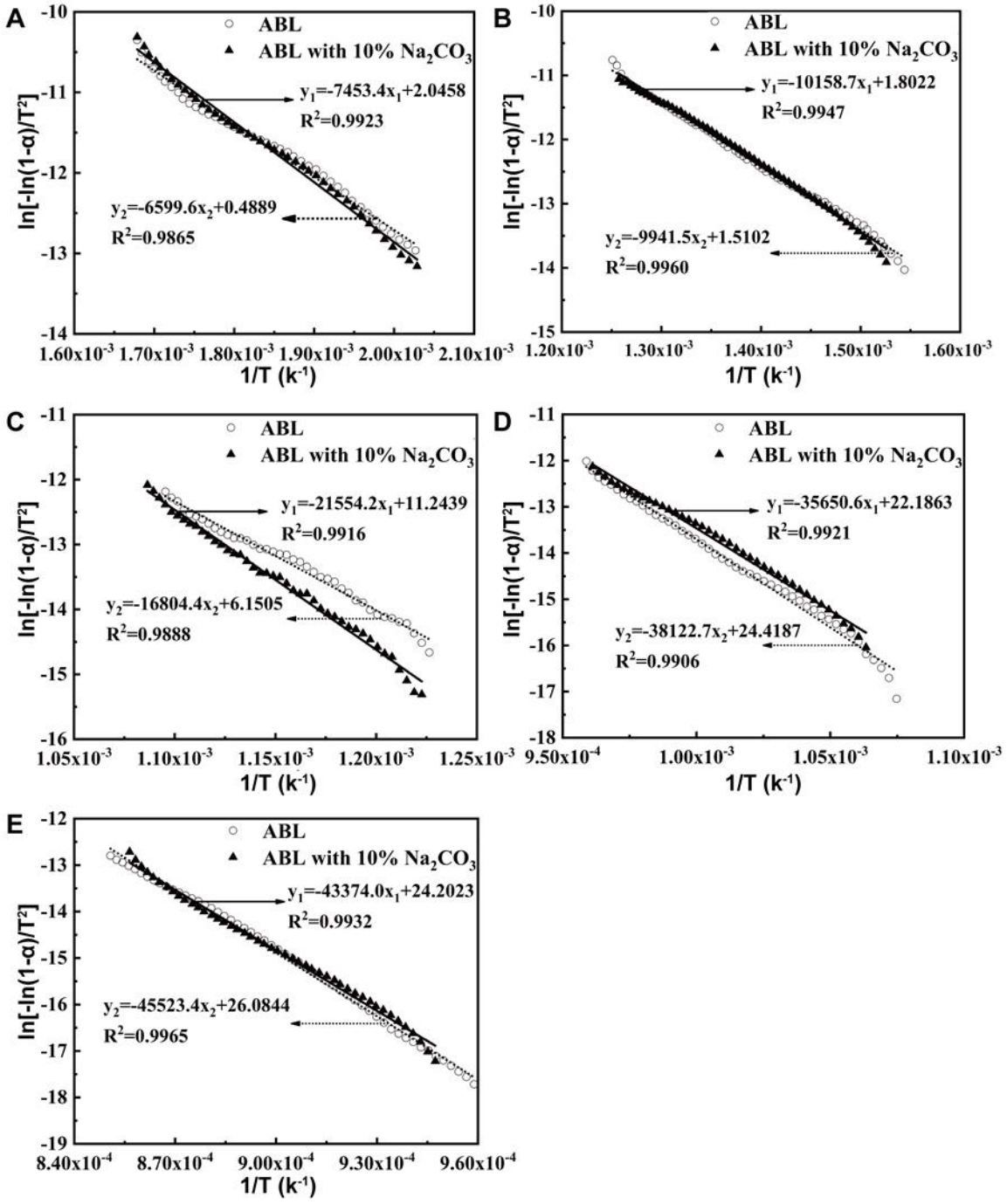

Fig. 3. Diagram of kinetic fitting of BABL-solids pyrolysis within various temperature ranges: (A) 217 °C to 360 °C; (B) 360 °C to 527 °C; (C) 527 °C to 650 °C; (D) 650 °C to 770 °C; (E) 770 °C to 900 °C.

The *E* of BABL-solids pyrolysis after adding 10% Na_2CO_3 decreased by 6.48% and 4.72% within 650 °C to 770 °C and 770 °C to 900 °C, respectively, as shown in Table 2. This indicated that Na_2CO_3 promoted BABL-solids pyrolysis within these temperature ranges.

Table 2. Activation Energies and Rate Changes of BABL-Solids Pyrolysis with Various Temperature Ranges

Ranges Temperature (°C)	$-\frac{E}{R}$		*E* (kJ/mol)		Rate Change[1] (%)
	BABL-solids	10% Na_2CO_3 addition	BABL-solids	10% Na_2CO_3 addition	
217 – 360	-6599.6	-7453.4	54.87	61.97	12.94
360 – 527	-9941.5	-10158.7	82.65	84.46	2.19
527 – 650	-16804.4	-21554.2	139.71	179.20	28.27
650 – 770	-38122.7	-35650.6	316.95	296.40	-6.48
770 – 900	-45523.4	-43374.0	378.48	360.61	-4.72

[1] Rate change is the percentage of the value of E-value of 10% Na_2CO_3 addition minus E-value of BABL-solids to E-value of BABL-solids.

Analysis of Surface Morphology

The BABL-solids are granular prior to pyrolysis, as shown in Fig. 4A. The granular particle were not observed, but the needle crystals and holes with various sizes were detected on BABL-solids surface after pyrolysis at 200 °C, as shown in Fig. 4B. The holes are the pores left by evaporation of steam from the dewatering of BABL-solids. The needle crystals were formed because of the result of recrystallization of inorganic matter, as the original BABL-solids were not found. It can be explained by the dewatering from BABL-solids, which caused a high humid environment to dissolve the inorganic matter, then dewater and recrystallize the material.

The surface of BABL-solids became compact and the holes disappeared after the BABL-solids pyrolysis at 400 °C (Fig. 4C). The entire surface became covered with a dense layer of minerals, indicating that the needle crystals were dissolved. The reasonable explanation may be that BABL-solids liquefaction process produced a high-humidity environment, which caused the hygroscopic dissolution of inorganic matter (NaOH and Na_2CO_3). The inorganic matter was dragged away from BABL-solids' surface by the rising steam produced by cracking of organic matter, and the steam quickly escaped at such a high temperature that the mineral deposits on the surface of the black liquor formed a dense layered structure. Expectedly, by this time, the BABL was also solidified.

The holes with different sizes are observed on the surface again, and plate-like species are also observed on BABL-solids surface after pyrolysis at 600 °C, as shown in Fig. 4D. These holes can be explained by the porous structure generated by the coking of organic matter. The layered structure is broken by the gas produced by the coking of the organic matter, causing a flake like structure.

The plate-like substances disappeared from the surface, and the number of holes were reduced after BABL-solids pyrolysis at 700 °C, as shown in Fig. 4E. This can be explained by melting of inorganic matter and filling the porous sites by char.

The size and cracks of microspores began to increase after BABL-solids pyrolysis at 800 °C, as shown in Fig. 4F. The char formation was catalyzed by Na_2CO_3, producing

CO, which caused the airflow to burst through the char. Consequently, the cracks appeared on the surface of BABL-solids char.

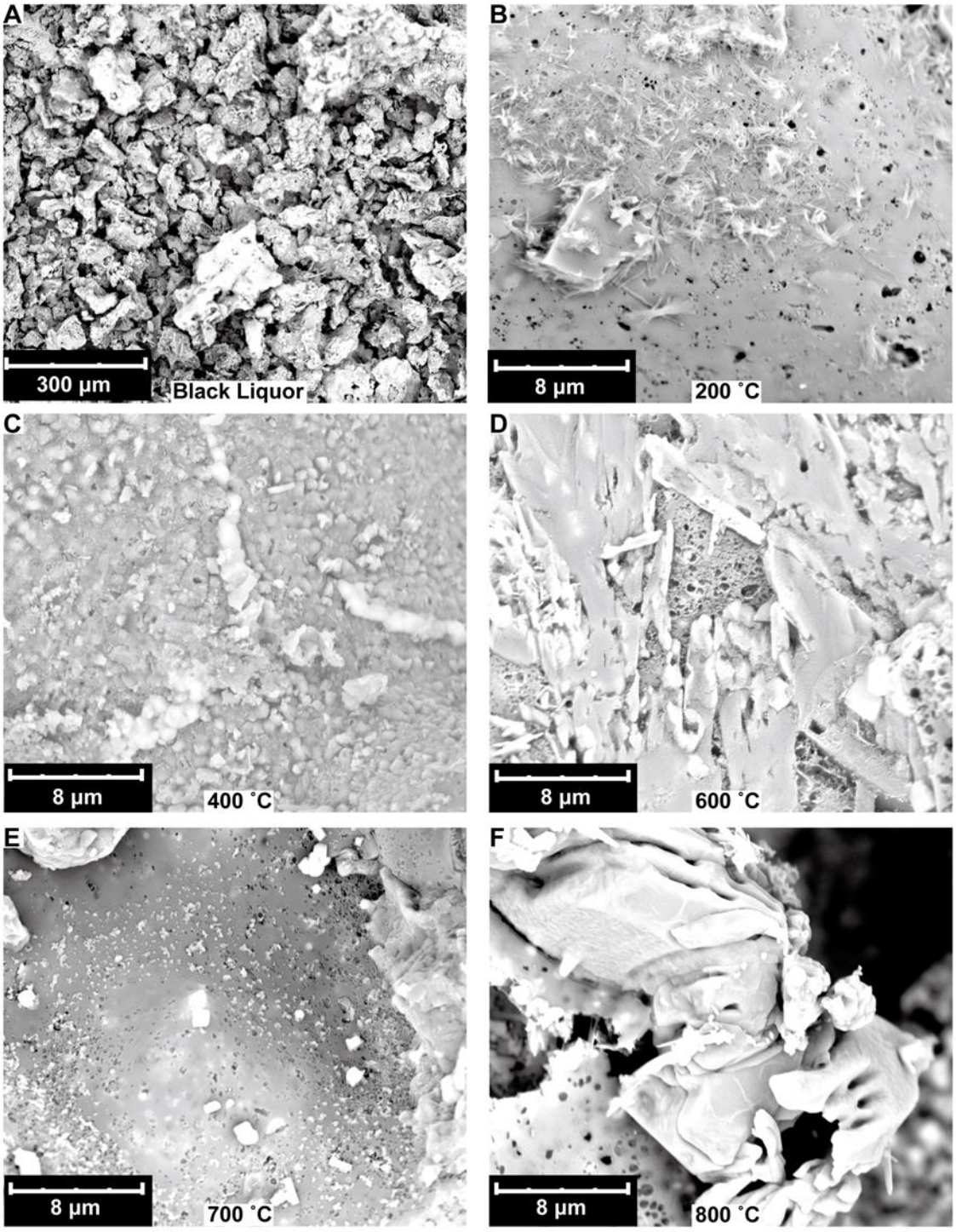

Fig. 4. SEM images of BABL-solids with 10% Na_2CO_3 surface at different temperature

CONCLUSIONS

1. The weight loss of BABL-solids pyrolysis occurred during the devolatilization stage (200 °C to 650 °C) and the reduction stage (650 °C to 1000 °C). The weight loss ratios of these two stages were 26.72% and 48.67%, respectively, in N_2 atmosphere at 10 K/min by TGA.
2. Weight loss was rapid in the devolatilization stage of BABL-solids pyrolysis and reduced slowly in the reduction stage of BABL-solids.
3. The Na_2CO_3 played both an inhibition and promotion role in the devolatilization stage and the reduction stage of the pyrolysis, respectively. Both inhibition and promotion became more prominent as the Na_2CO_3 addition ratio was increased.
4. The role of Na_2CO_3 on BABL-solids pyrolysis was related to its structure and state present in BABL-solids. Adding Na_2CO_3 tends to increase the thickness of the salt layer, which increased the activation energy and reduced the weight loss ratio of BABL-solids pyrolysis within 200 °C to 650 °C. Adding Na_2CO_3 increased the number of alkaline compounds or the active sites of the reduction reaction, which reduced the activation energy and increased the weight loss ratio of BABL-solids pyrolysis within 650 °C to 1000 °C.
5. The final weight loss ratio of BABL-solids pyrolysis increased as the Na_2CO_3 addition ratio was increased. The benefit was available without additional investment, since Na_2CO_3 is a by-product of black liquor gasification.

ACKNOWLEDGMENTS

This project was sponsored by research funds from the Guangxi Key Laboratory of Clean Pulp and Papermaking, and Pollution Control (ZR201605). The authors are grateful for the financial support from the Guangxi Key Laboratory of Clean Pulp and Papermaking, Pollution Control and the Guangxi Natural Fund.

Conflict of Interest

The authors declare no conflict of interest.

REFERENCES CITED

Abdelfattah, M. S. H., Abu-Elyazeed, O. S. M., Abd El Mawla, E., and Abdelazeem, M. A. (2018). "On biodiesels from castor raw oil using catalytic pyrolysis," *Energy* 143, 950-960. DOI: 10.1016/j.energy.2017.09.095

Alén, R., Rytkönen, S., and McKeough, P. (1995). "Thermogravimetric behavior of black liquors and their organic constituents," *Journal of Analytical and Applied Pyrolysis* 31, 1-13. DOI: 10.1016/0165-2370(94)00811-E

Beis, S. H., Mukkamala, S., Hill, N., Joseph, J., Baker, C., Jensen, B., Stemmler, E. A., Wheeler, M. C., Frederick, B. G., and Heiningen, A. V. J. B. (2010). "Fast pyrolysis of lignins," *BioResources,* 5(3), 1408-1424. DOI: 10.15376/biores.5.3.1408-1424

Bradbury, A. G., Sakai, Y., and Shafizadeh, F. J. (1979). "A kinetic model for pyrolysis of cellulose," *Journal of Applied Polymer Science* 23(11), 3271-3280. DOI: 10.1002/app.1979.070231112

Chu, J. Y., Jiang, W. K., and Wu, S. B. (2017). "Depolymerization characteristics during the pyrolysis of two industrial lignins," *BioResources*, 12(4), 7241-7254. DOI: 10.15376/biores.12.4.7241-7254

Demuner, I. F., Colodette, J. L., Demuner, A. J., and Jardim, C. M. (2019). "Biorefinery review: Wide-reaching products through kraft lignin," *BioResources* 14(3), 7543-7581. DOI: 10.15376/biores.14.3. 7543-7581

Ebrahimi-Kahrizsangi, R., and Abbasi, M. H. (2008). "Evaluation of reliability of Coats-Redfern method for kinetic analysis of non-isothermal TGA". *Transactions of Nonferrous Metals Society of China,* 18(1), 217-221. DOI: 10.1016/S1003-6326(08)60039-4

Evans, R., and Milne, T. (1988). "Pyrolysis oils from biomass: Producing, analyzing, and upgrading," *American Chemical Society (ACS) Symposium Series*. pp. 311-327.

Farzaneh, A., Richards, T., Sklavounos, E., and van Heiningen, A. (2014). "A Kinetic study of CO_2 and steam gasification of char from lignin produced in the sew process," *BioResources*, 9(2), 3052-3063. DOI: 10.15376/biores.9.2. 3052-3063

Gea, G., Murillo, M. B., and Arauzo, J. (2002). "Thermal degradation of alkaline black liquor from straw. Thermogravimetric study," *Industrial & engineering chemistry research* 41(19), 4714-4721. DOI: 10.1021/ie020283z

Gea, G., Murillo, M. B., Sanchez, J. L., and Arauzo, J. (2003). "Thermal degradation of alkaline black liquor from wheat straw. 2. Fixed-bed reactor studies," *Industrial* and *Engineering Chemistry Research* 42(23), 5782-5790. DOI: 10.1021/ie030116e

Gea, G., Sanchez, J. L., Murillo, M. B., and Arauzo, J. (2005). "Kinetics of CO_2 gasification of alkaline black liquor from wheat straw. 2. Evolution of CO_2 reactivity with the solid conversion and influence of temperature on the gasification rate," *Industrial and Engineering Chemistry Research* 44(17), 6583-6590. DOI: 10.1021/ie048772h

Guo, D. L., Wu, S. B., Lou, R., Yin, X. L., and Yang, Q. (2011). "Effect of organic bound Na groups on pyrolysis and CO_2-gasification of alkali lignin," *BioResources* 6(4), 4145-4157. DOI: 10.15376/biores.6.4. 4145-4157

Guo, D. L., Wu, S. B., Liu, B., Yin, X. L., and Yang, Q. (2012). "Catalytic effects of NaOH and Na_2CO_3 additives on alkali lignin pyrolysis and gasification," *Applied Energy 95*, 22-30. DOI: 10.1016/j.apenergy.2012.01.042

Gustafsson, C., and Richards, T. (2009). "Pyrolysis kinetics of washed precipitated lignin," *BioResources* 4(1), 26-37. DOI:10.15376/biores.4.1.26-37

Huang, H. J., and Ramaswamy, S. (2011). "Thermodynamic analysis of black liquor steam gasification," *BioResources* 6(3), 3210-3230. DOI: 10.15376/biores.6.3. 3210-3230

Hubbe, M. A., Alen, R., Paleologou, M., Kannangara, M., and Kihlman, J. (2019). "Lignin Recovery from spent alkaline pulping liquors using acidification, membrane separation, and related processing steps: A review," *BioResources* 14(1), 2300-2351. DOI: 10.15376/biores.14.1.2300-2351

Jensen, F. (1985). "Activation energies and the Arrhenius equation," *Quality and Reliability Engineering International* 1(1), 13-17. DOI: 10.1002/qre.4680010104

Li, J., and van Heiningen, A. (1990) of Conference. "Sodium emission during pyrolysis and gasification of black liquor char," *Pulping Conference:[proceedings](USA)*.

Li, J., van Heiningen, A. R. (1991). "Kinetics of gasification of black liquor char by steam," *Industrial and Engineering Chemistry Research* 30(7), 1594-1601. DOI: 10.1021/ie00055a027

Li, X. H., and Wu, S. B. (2014). "Chemical Structure and pyrolysis characteristics of the soda-alkali lignin fractions," *BioResources* 9(4), 6277-6289. DOI: 10.15376/biores.6.3.6277-6289

Lora, J. (2008). "Industrial commercial lignins: sources, properties and applications," In: *Monomers, Polymers and Composites from Renewable Resources*, Elsevier, pp. 225-241. DOI: 10.1016/B978-0-08-045316-3.00010-7

Naqvi, M., Yan, J., and Dahlquist, E. (2010). "Black liquor gasification integrated in pulp and paper mills: A critical review," *Bioresource Technology* 101(21), 8001-8015. DOI: 10.1016/j.biortech.2010.05.013

Naqvi, S. R., Uemura, Y., Osman, N., and Yusup, S. (2015). "Kinetic study of the catalytic pyrolysis of paddy husk by use of thermogravimetric data and the Coats-Redfern model," *Research on Chemical Intermediates* 41(12), 9743-9755. DOI: 10.1007/s11164-015-1962-0

Nguyen, T. S., He, S. B., Raman, G., and Seshan, K. (2016). "Catalytic hydro-pyrolysis of lignocellulosic biomass over dual Na_2CO_3/Al_2O_3 and Pt/Al_2O_3 catalysts using n-butane at ambient pressure," *Chemical Engineering Journal* 299, 415-419. DOI: 10.1016/j.cej.2016.04.104

Peng, W. X., Ge, S. B., Ebadi, A. G., Hisoriev, H., and Esfahani, M. J. (2017). "Syngas production by catalytic co-gasification of coal-biomass blends in a circulating fluidized bed gasifier," *Journal of Cleaner Production* 168, 1513-1517. DOI: 10.1016/j.jclepro.2017.06.233

Song, X. F., Bie, R. S., Ji, X. Y., Chen, P., Zhang, Y., and Fan, J. (2015). "Kinetics of reed black liquor (rbl) pyrolysis from thermogravimetric data," *BioResources* 10(1), 137-144. DOI: 10.15376/biores.10.1.137-144

Sricharoenchaikul, V., Frederick, W. J., and Agrawal, P. (2002). "Black liquor gasification characteristics. 1. Formation and conversion of carbon-containing product gases," *Industrial and Engineering Chemistry Research* 41(23), 5640-5649. DOI: 10.1021/ie020207w

Whitty, K., Kullberg, M., Sorvari, V., Backman, R., and Hupa, M. J. B. T. (2008). "Influence of pressure on pyrolysis of black liquor: 2. Char yields and component release," *Bioresource technology* 99(3), 671-679. DOI: 10.1016/j.biortech.2006.11.064

Yigezu, Z. D., and Muthukumar, K. (2014). "Catalytic cracking of vegetable oil with metal oxides for biofuel production," *Energy Conversion and Management* 84, 326-333. DOI: 10.1016/j.enconman.2014.03.084

Yu, H. M., Wu, Z. L., and Chen, G. (2018). "Catalytic gasification characteristics of cellulose, hemicellulose and lignin," *Renewable Energy* 121, 559-567. DOI: 10.1016/j.renene.2018.01.047

Zhenqiu, L., and Kefu, C. (2000). "Pyrolysis Behaviour of bagasse pulping black liquor," *Transactions of China Pulp and Paper,* S1.

Article submitted: November 15, 2019; Peer review completed: January 23, 2019; Revisions accepted: February 6, 2020; Published: February 11, 2020.
DOI: 10.15376/biores.15.2.2428-2441